

Tensor correlation in ^4He with the tensor-optimized shell model

Takayuki MYO,^{1,*} Satoru SUGIMOTO,^{2,**} Kiyoshi KATŌ^{3***} Hiroshi TOKI,^{1†}
and Kiyomi IKEDA^{4††}

¹*Research Center for Nuclear Physics (RCNP), Osaka University, Ibaraki
567-0047, Japan*

²*Department of Physics, Graduate School of Science, Kyoto University, Kyoto
606-8502, Japan*

³*Division of Physics, Graduate School of Science, Hokkaido University, Sapporo
060-0810, Japan*

⁴*The Institute of Physical and Chemical Research (RIKEN), Wako 351-0198,
Japan.*

(Received December 2, 2024)

We study the characteristics of the tensor correlation in ^4He in the shell model type method. We treat the tensor force explicitly by performing a configuration mixing calculation in the $2p2h$ basis and take single-particle states up to medium high angular momenta. We adopt the Gaussian expansion method for the quantitative description of the spatial shrinkage of the single-particle states to optimize the tensor correlation. We could describe full strength of the tensor correlation for ^4He in the shell model type method by achieving the convergence. We call this model as tensor-optimized shell model. It is found that in ^4He , three specific $2p2h$ configurations are strongly coupled with the $(0s)^4$ configuration due to the characteristic feature of the tensor operator.

§1. Introduction

The tensor force is an essential component in nuclear force and plays a significant role in the nuclear structure. For ^4He accurate calculations using realistic nucleon-nucleon interaction demonstrated that the contribution of the tensor force is very large to reach about -68 MeV, which is the same order or even larger than that of the central force.^{1)–3)} The resulting strong tensor correlation enhances the D -state probability up to about 15% in the wave function. In light nuclei up to around mass number 10 ($A \leq 10$), the Green's function Monte Carlo (GFMC) method⁴⁾ was developed to treat the realistic interaction and was able to describe ground states and a few excited states. There it was demonstrated that the contribution of the one-pion exchange potential (OPEP) provides 70% \sim 80% of the two-body attraction, where the dominant component of OPEP is the tensor force.

We definitely want to describe nuclei with larger mass numbers using explicitly the realistic nucleon-nucleon interaction. The variational methods including GFMC

*) E-mail : myo@rcnp.osaka-u.ac.jp

**) E-mail : satoru@ruby.scphys.kyoto-u.ac.jp

**) E-mail : kato@nucl.sci.hokudai.ac.jp

†) E-mail : toki@rcnp.osaka-u.ac.jp

††) E-mail : k-ikeda@postman.riken.go.jp

of a few-body system use the relative coordinates of nucleons, which are suitable to work out the nucleon-nucleon interaction. We shall call this as the many-body theory with T -type basis, since the two interacting nucleons, whose center of mass is connected with some reference coordinate, are directly connected by the nucleon-nucleon interaction. In this case, the number of the relative coordinates increase with $A(A-1)/2$, where A is the number of nucleons. Hence, the T -type basis is not suited for heavier systems and calculations become increasingly difficult with N . On the other hand, the mean-field framework uses the coordinates of nucleons from the center of the nucleus, where the number of the coordinates is N and hence suited for heavy systems. We shall call this method as the many-body theory with V -type basis, since the two interacting nucleons are expressed by the coordinates from the center of the nucleus and indirectly connected with the nucleon-nucleon interaction. Hence it is difficult to treat the realistic interaction involving the short-range repulsion and the tensor force, because many configuration in the V -type basis are needed to describe the motion under such a realistic interaction. In this case, we have to invent some method to treat these features of the realistic interaction.

The standard method of the description of many-body systems in the V -type basis is the Brueckner-Hartree-Fock (BHF) method,⁵⁾⁻⁷⁾ in which two-body interaction with the short-range repulsion and the strong tensor force is treated by the Brueckner G -matrix effective interaction under the independent pair approximation. Since the resulting G -matrix effective interaction is a smooth interaction, the wave functions in the V -type basis can treat the G -matrix within the model space. The BHF method or the shell model, which is based on the concept of the Brueckner theory, have a certain success in description of many-body systems. However, there seems some essential feature as the spin-orbit interaction missing^{8),9)} and we are forced to take some phenomenology.

Recently there were two important steps proposed for the full description of nuclei in the V -type basis. One is the proposal of Neff and Feldmeier in terms of the unitary transformation of the radial correlation due to the short-range repulsion and the tensor correlation due to the tensor force separately.¹⁰⁾ The unitary transformation method introduces the unitary operator for the short-range repulsion and another unitary operator for the tensor force. The short-range repulsion seems treated properly, since the short-range repulsion works at a very small distance ($r \leq 0.5$ fm) and therefore the terms more than the three-body operators caused by the radial unitary transformations could be neglected.¹¹⁾ On the other hand, the tensor force are not treated properly within the two-body terms of the unitary transformed Hamiltonian. This may be related with the fact that the range of the tensor force is intermediate ($0.5 \text{ fm} \leq r \leq 1.4 \text{ fm}$).

The other is the proposal of Toki *et al.*¹²⁾ for the treatment of the pion exchange interaction in terms of the relativistic mean-field framework. The mean-field method was introduced in the relativistic mean-field approximation with the finite pion mean field. Since the pion is the pseudo-scalar meson, the finite pion mean field in the spherical ansatz naturally induces the parity mixing of the intrinsic single-particle states. This relativistic mean-field model provides an interesting mechanism for the splitting of the spin-orbit partner due to the mixture of the parity partners with

the same total spin as $s_{1/2}$ and $p_{1/2}$ or $p_{3/2}$ and $d_{3/2}$.¹³⁾ This work gave us a hint of taking the parity mixing single-particle states for the description of the tensor correlation in the non-relativistic approximation. Furthermore, it is straightforward to perform the parity projection and also the charge projection due to the fact that the tensor force is isospin dependent.¹⁴⁾ The leading term of the parity and charge projection is $2p2h$ configurations.¹²⁾

Hence, the next step was to take the shell model type prescription where the closed shell wave function is treated as the $0p0h$ state and $2p2h$ wave functions are introduced to treat the tensor force.¹⁵⁾ When this method was applied to ${}^4\text{He}$, where the closed shell state is $(0s_{1/2})^4$ and the particle states of the $2p2h$ configurations are those in the p -orbit, the major $2p2h$ state turned out to be $(0p_{1/2})^2(0s_{1/2})^{-2}$, the pionic state, and the spatial extension of the $0p_{1/2}$ wave function is shrunk by almost a half of the ordinary harmonic oscillator wave function.¹⁵⁾ In this case, however, we still had to enhance the matrix element of the tensor force by 50% in order to provide enough amount of the D -state probability of ${}^4\text{He}$. We have to understand why we ought to increase the tensor matrix element by 50%.

In this paper, we would like to extend further the shell model type method by increasing the $2p2h$ configurations in order to understand the origin of the 50% increase of the tensor matrix element. We shall think more the characteristics of the tensor force. The tensor force is $V_T = f_T(r)S_{12}$ with the tensor operator, $S_{12} = \sqrt{24\pi}[Y_2(\hat{r}_{12}), [\boldsymbol{\sigma}^1, \boldsymbol{\sigma}^2]_2]_0$. Both of the spins of two particles have to flip by unit of two, $\Delta S = 2$, and the orbital angular momentum by two, $\Delta L = 2$. Hence, the lowest relative angular momentum state is the $L = 2$ state, where the centrifugal potential behaves as $V_{cen} = 6\hbar^2/(m_N r^2)$ and it is 1 GeV at 0.5 fm. This means we ought to describe the distance as short as about 0.5 fm and larger by introducing higher angular momentum states. We have the relation, $f_T(r) = \sum_l f_l(r_1, r_2)P_l(\hat{r}_{12})$. Here, $P_l(\hat{r}_{12})$ has a significant strength around $\hat{r} \sim 0$ with the width of about $1/l$ for large l ($l \geq 5$). We can write $P_l(\hat{r}_{12}) = (4\pi/\sqrt{2l+1})(-)^l[Y_l(\hat{r}_1), Y_l(\hat{r}_2)]_0$. Since the relative distance to be expressed by the high-spin state with l of the V -type coordinate is $r_1 \times (1/l) \geq 0.5$ fm with $r_1 \sim r_2 \sim 2$ fm (the size of ${}^4\text{He}$), we find $l \leq 4$. In addition, there is the additional change of the angular momentum by two for the case of the tensor force. This means that we may be able to describe the tensor matrix element by taking the single-particle states with angular momentum up to $l = 4 + 2 = 6$ for the ${}^4\text{He}$ case. Hence, we may be able to describe the tensor force in terms of the V -type coordinates with medium size angular momenta. It remains to construct a shell model type prescription to handle the tensor force by using the V -type basis. We name this model as tensor optimized shell model.

The tensor optimized shell model (TOSM) is described as follows.

- (1) We base on the closed shell state as the $0p0h$ state and add $2p2h$ states.
- (2) We include medium high angular momentum orbits for the particle states within the $2p2h$ excitations.
- (3) We allow radial shrinkage of the particle states by taking the Gaussian wave function with the lowest node for each angular momentum state.
- (4) We take the many-body Hamiltonian with suitably chosen two-body interaction

including explicitly the tensor force.

As for ${}^4\text{He}$, we take the $(0s_{1/2})^4$ state as the basic state and take $2p2h$ states with the particle states of finite angular momenta as large as the result converges with the expectation of the convergence around $l = 6$. All the angular momentum states have no node except the one of the s -state, which is constructed as an orthogonal state with the $0s$ state with Gaussian wave functions with various size parameters. As for the short-range repulsion, we do not touch on this problem in this paper and take just a phenomenologically available one. However, once we succeed the description of the tensor force, we shall work out the short-range part in the future.

In §2, we describe in detail the tensor-optimized shell model (TOSM), which treats the tensor correlation explicitly. In §3 we investigate the structure of ${}^4\text{He}$ by taking high angular momentum states, and discuss the characteristics of the tensor correlation. In §4, we discuss the tensor correlation in detail in terms of the radial shrinkage with the Gaussian expansion method. In §5, we calculate ${}^4\text{He}$ by taking the bare tensor force of AV8' with a slight modification of the central interaction in the TOSM. The present study is summarized in §6.

§2. Tensor optimized shell model for ${}^4\text{He}$

In this paper, we apply the tensor optimized shell model to ${}^4\text{He}$. Particularly, we would like to see if the tensor correlation is satisfactorily described by taking Gaussian wave functions with medium size angular momenta.

2.1. Higher partial waves and variational methods

We base $2p2h$ wave functions on the closed shell wave function as the $0p0h$ state and take the $(0s_{1/2})^4$ state for ${}^4\text{He}$. We take $2p2h$ excitations with higher partial waves up to l_{max} where l_{max} is the maximum orbital angular momentum of the excited particle orbits. We successively increase the value of l_{max} to see the convergence of the solutions. The $1s$ orbit is included in the cases of $l_{max} \geq 2$. We describe the particle states with keeping their orthogonality to the occupied states. We do not include higher nodal orbits such as $2s$, $1p$ except for the $1s$ orbit. This is because we check that the usual shell model type calculation including the higher nodal orbits of harmonic oscillator wave functions (HOWF) with a common length parameter is difficult to describe the tensor correlation satisfactorily. In fact, the tensor correlation was investigated using the higher nodal HOWF in the old study,¹⁶⁾ and it was shown that the convergence of the solutions with respect to the principal quantum number N was slow. Furthermore, we learned that the tensor correlation is optimized with the small size parameters of Gaussian wave functions for the excited particle states. These results mean that the ordinary HOWF is not enough to represent the tensor correlation sufficiently. Instead of HOWF, we adopt the Gaussian expansion technique^{17),18)} for single-particle orbits. Each Gaussian basis function has a form of the nodeless HOWF except for $1s$ orbit and when we superpose a sufficient number of Gaussian basis functions with adequate length parameters, we can fully optimize the radial component of every orbit.

The form of the Gaussian basis function for the label α such as $0s_{1/2}$ and $0p_{1/2}$,

is expressed as follows

$$\phi_\alpha(\mathbf{r}, b_{\alpha,m}) = N_l(b_{\alpha,m}) r^l e^{-(r/b_{\alpha,m})^2/2} [Y_l(\hat{\mathbf{r}}), \chi_{1/2}]_j, \quad (2.1)$$

$$N_l(b_{\alpha,m}) = \left[\frac{2 b_{\alpha,m}^{-(2l+3)}}{\Gamma(l+3/2)} \right]^{\frac{1}{2}}, \quad (2.2)$$

where m is an index to distinguish the Gaussian basis function with different length parameter $b_{\alpha,m}$. We construct the following ortho-normalized single-particle wave function ψ_α^n with linear combination of the Gaussian bases

$$\psi_\alpha^n(\mathbf{r}) = \sum_{m=1}^{N_\alpha} d_{\alpha,m}^n \phi_\alpha(\mathbf{r}, b_{\alpha,m}), \quad \text{for } n = 1, \dots, N_\alpha, \quad (2.3)$$

where N_α is a number of the basis functions for α . The coefficients $\{d_{\alpha,m}^n\}$ are determined by solving the eigenvalue problem for the norm matrix of the non-orthogonal Gaussian basis set in Eq. (2.1). We obtain the new single-particle wave functions $\{\psi_\alpha^n\}$ in Eq. (2.3) which are distinguished by an index n for the different radial component in the same label α .

We set the Gaussian basis functions for the particle states to be orthogonal to the occupied single-particle states, which are $0s_{1/2}$ in the case of ${}^4\text{He}$. For $0s_{1/2}$ states, we simply employ one Gaussian basis function, namely, HOWF with length $b_{0s_{1/2},m=1} = b_{0s}$. For $1s_{1/2}$ states, we introduce the orthogonal basis to the $0s_{1/2}$ states and has a different length parameter $b_{1s,m}$ from b_{0s} . This extended $1s_{1/2}$ state is expressed as follows

$$\begin{aligned} \phi_{1s}(\mathbf{r}, b_{0s}, b_{1s,m}) &= N(b_{1s,m}) \{f_0(b_{0s}, b_{1s,m}) + f_2(b_{0s}, b_{1s,m}) r^2\} \\ &\times e^{-(r/b_{1s,m})^2/2} Y_{00}(\hat{\mathbf{r}}), \end{aligned} \quad (2.4)$$

where we omit writing the spin wave function. The coefficients f_0 and f_2 are determined by the normalization of ϕ_{1s} and the orthogonality to the $0s$ state. The ortho-normalized $1s$ wave functions $\{\psi_{1s}^n\}$ are obtained from ϕ_{1s} with various range parameters as described above.

Here we set the variational wave function for ${}^4\text{He}$. Each configuration of ${}^4\text{He}$ is expressed by the anti-symmetrized products of the four single-particle states which are distinguished by α and basis index n as follows

$$\Phi_p = \mathcal{A} \left\{ \prod_{k=1}^4 \psi_{\alpha_k}^{n_k} \right\}, \quad (2.5)$$

where p indicates the set of $\{\alpha_k, n_k; k = 1, \dots, 4\}$. The total wave function of ${}^4\text{He}$ with $(J^\pi, T) = (0^+, 0)$ for spin and isospin is expressed by a superposition of Φ_p as

$$\Psi({}^4\text{He}) = \sum_p a_p \Phi_p, \quad (2.6)$$

where a_p is variational coefficients.

The variation of the energy expectation value with respect to the total wave function $\Psi(^4\text{He})$ is given by

$$\delta \frac{\langle \Psi | H | \Psi \rangle}{\langle \Psi | \Psi \rangle} = 0 , \quad (2.7)$$

which leads to the following equations:

$$\frac{\partial \langle \Psi | H - E | \Psi \rangle}{\partial b_{\alpha,m}} = 0 , \quad \frac{\partial \langle \Psi | H - E | \Psi \rangle}{\partial a_p} = 0 . \quad (2.8)$$

Here, E is a Lagrange multiplier corresponding to the total energy. The parameters $\{b_{\alpha,m}\}$ for the Gaussian bases appear non-linearly in the energy expectation value. We solve these two kinds of variational equations in the following steps. First, fixing all the length parameters $b_{\alpha,m}$, we solve the linear equation for $\{a_p\}$ as an eigenvalue problem for H with partial waves up to l_{max} . We obtain the eigenvalue E which is a function of $\{b_{\alpha,m}\}$. Next, we try various sets of the length parameters $\{b_{\alpha,m}\}$ in order to find the solution which minimizes the total energy. In this wave function, we can describe the spatial shrinkage with an appropriate radial form, which is important for the tensor correlation.

In this paper, we have two steps of the analysis. First is the main analysis in which we prepare a single Gaussian basis function for each label α ($N_\alpha = 1$ in Eq. (2.3)). In this case, we discuss the convergence of the energy by including higher partial waves and investigate the characteristics of the configuration mixing. Second, we adopt the Gaussian expansion method for the excited nucleon states and examine the quantitative description of spatial shrinkage of the wave function.

Our wave function may contain the excitation of the spurious center of mass (c.m.) motion. We estimate this amount using a following operator H_G .

$$H_G = T_G + \frac{1}{2} M_G \omega^2 \mathbf{R}_G^2, \quad T_G = \frac{\mathbf{P}_G^2}{2M_G} \quad (2.9)$$

$$M_G = A \cdot m_N, \quad \mathbf{R}_G = \frac{1}{A} \sum_{i=1}^A \mathbf{r}_i, \quad \mathbf{P}_G = \sum_{i=1}^A \mathbf{p}_i, \quad \omega = \frac{\hbar}{m_N b_{0s}^2}, \quad (2.10)$$

where A is a mass number. When the c.m. motion is constrained to the $0s$ state in the total wave function, $\langle H_G \rangle$ must be $1.5 \hbar \omega$. We estimate the amount of the spurious c.m. motion from the deviation of $\langle H_G \rangle$ with respect to $1.5 \hbar \omega$.

2.2. Hamiltonian

The Hamiltonian for ^4He is given by

$$H = \sum_{i=1}^4 t_i - T_G + \sum_{i<j}^4 v_{ij} , \quad (2.11)$$

with

$$v_{ij} = v_{ij}^C + v_{ij}^T + v_{ij}^{LS} + v_{ij}^{Cmb} . \quad (2.12)$$

The effective NN interaction v_{ij} consists of central (v_{ij}^C), tensor (v_{ij}^T), LS (v_{ij}^{LS}) and Coulomb (v_{ij}^{Cmb}) terms. We do not explicitly treat the short-range correlation and use some phenomenological central interactions. As for the tensor force, we use one of the effective tensor force in which the short-range part is renormalized as it has been the standard choice for our study of the tensor correlation. We will demonstrate toward the end of this paper, however, that the tensor correlation does not depend on the effective tensor interaction qualitatively, because of the strong centrifugal potential.¹⁵⁾

We explain effective interactions that include the tensor force explicitly and suitable for the present analysis. We use a sufficiently strong tensor force comparable to the realistic interaction, since we would like to learn the characteristics of the tensor correlation in the structure of ${}^4\text{He}$. In Ref. 15), we examined two kinds of effective interaction, AK^{19),20)} and GPT.²¹⁾ AK is constructed from the AV8' realistic interaction using the G -matrix theory, where the cut off momentum for the Q -space for the G -matrices is chosen as $k_Q = 2.8 \text{ fm}^{-1}$, twice of the usual Fermi momentum ($k_F = 1.4 \text{ fm}^{-1}$). In this prescription, short-range correlations including very high momentum components ($k > k_Q$) of the tensor correlations are renormalized into the central term of the G -matrices. The tensor force giving the momentum components with $k < k_Q$ in the G -matrices survives in the intermediate- and long-ranges.^{19),20)} In fact, the matrix element of the tensor force given by AK is very close to that by the bare case (AV8'), which is discussed later in §5. We also refer to the so-called GPT interaction,²¹⁾ which has a mild short-range repulsion and is constructed to reproduce the two-nucleon properties. In GPT, renormalization of the tensor force is considered to be based on the conventional approach, which gives a weak tensor force.

We found that AK gives a large tensor contribution in ${}^4\text{He}$ ¹⁵⁾ and seems to be suitable for the present model to investigate the tensor correlation. However, as will be shown later, this force gives a small radius and an overbinding problem for ${}^4\text{He}$. Contrastingly, GPT gives a good radius and a good binding energy, but a small tensor contribution.¹⁵⁾ It is necessary to construct other appropriate interactions that take into account the short-range and tensor correlations consistently for the present model. This is, however, beyond the task of the present paper. In this study, we phenomenologically improve AK with the central part of AK replaced by that of GPT, and call this interaction GA. With this interaction, the total energy was good and the radius was improved in ${}^4\text{He}$.¹⁵⁾ Thus, GA is regarded as phenomenological effective interaction and we use this interaction to study the tensor correlation for ${}^4\text{He}$.

§3. Results of tensor correlation in the TOSM

We present here the results of the configuration mixing in TOSM and the contributions of higher angular momentum states for the tensor correlation in ${}^4\text{He}$. We show first the calculated results with partial waves up to $l_{max}=1$ to 6, with single Gaussian basis ($N_\alpha = 1$) for each single-particle state ψ_α , where we optimize the

length parameters of the Gaussian basis $\{b_{\alpha,m=1}\} = \{b_{\alpha}\}$ for every state. We also show the characteristic feature of the tensor correlation.

3.1. The calculated results with medium high angular momentum states

We here show the results of the energy minimum point in each case of l_{max} . The results for the set of $\{b_{\alpha}\}$ are listed in Tables I and for the properties of the ${}^4\text{He}$ wave functions in Table II. From Table I, the energy minima are obtained at around $b_{\alpha \neq 0s} \sim 0.6 b_{0s}$, which means the spatial shrinkage of the wave function. As will be discussed later, the expectation value of the tensor force $\langle V_T \rangle$ gives the largest contribution around this energy minimum.

From Table II and Fig. 1, with l_{max} we see the convergence of the energy, the central force contribution $\langle V_C \rangle$, $\langle V_T \rangle$, and the D -state probability $P(D)$. Here, we define $P(D)$ as the component in which the values of total orbital angular momentum and total spin are both two in the total wave function of $\Psi({}^4\text{He})$ in Eq. (2.6). It is also found that the convergence of $\langle V_T \rangle$ is slower than $\langle V_C \rangle$. This means that the higher partial waves are rather needed for the tensor correlation. For $\langle V_T \rangle$ and $P(D)$, the $l_{max} = 4$ case is almost enough in the present model. The excitation of the spurious c.m. motion is small as judged from the values of $\langle H_G \rangle$ and decreases with l_{max} as shown in Table II.

In Table III, we show the six configurations in the order of those probabilities for each case of l_{max} . For $2p2h$ states, excited two particle states are shown. The subscripts 00, 01, 10 or 11 represent J and T , spin and isospin for the two-nucleon pair, respectively. It is found that the three-kinds of $2p2h$ configurations with $(0p_{1/2})^2_{10}$, $[(1s_{1/2})(0d_{3/2})]_{10}$ and $[(0p_{3/2})(0f_{5/2})]_{10}$ for the particle part are significantly mixed. They have common values of $(J, T) = (1, 0)$ which are the same as those of deuteron, and this two-nucleon coupling is understood as a deuteron-like correlation.¹⁵⁾

In order to see the relation between those three configurations and the tensor correlation, we expand $\langle V_T \rangle$ into two terms of matrix elements between $0p0h$ and

Table I. The optimized length parameters of single-particle states for ${}^4\text{He}$ in unit of fm.

l_{max}	$0s_{1/2}$	$0p_{1/2}$	$0p_{3/2}$	$1s_{1/2}$	$0d_{3/2}$	$0d_{5/2}$	$0f_{5/2}$	$0f_{7/2}$
1	1.26	0.75	0.69	—	—	—	—	—
2	1.19	0.78	0.75	0.76	0.69	0.62	—	—
3	1.16	0.74	0.66	0.73	0.67	0.62	0.77	0.66
4	1.16	0.75	0.67	0.73	0.67	0.61	0.77	0.67
5	1.16	0.76	0.67	0.73	0.67	0.61	0.77	0.64
6	1.16	0.76	0.67	0.73	0.67	0.61	0.77	0.64
l_{max}	$0g_{7/2}$	$0g_{9/2}$	$0h_{9/2}$	$0h_{11/2}$	$0i_{11/2}$	$0i_{13/2}$		
4	0.70	0.67	—	—	—	—		
5	0.70	0.68	0.70	0.67	—	—		
6	0.70	0.67	0.70	0.69	0.71	0.65		

$2p2h$ components and between $2p2h$ and $2p2h$ ones as follows

$$\langle V_T \rangle = \sum_{p,p'} a_p a_{p'} \langle \Phi_p | V_T | \Phi_{p'} \rangle = \{0p0h-2p2h\} + \{2p2h-2p2h\}, \quad (3.1)$$

$$\{0p0h-2p2h\} \equiv \sum_{p \in 2p2h} a_{0p0h} a_p (\langle \Phi_{0p0h} | V_T | \Phi_p \rangle + \langle \Phi_p | V_T | \Phi_{0p0h} \rangle), \quad (3.2)$$

$$\{2p2h-2p2h\} \equiv \sum_{p,p' \in 2p2h} a_p a_{p'} \langle \Phi_p | V_T | \Phi_{p'} \rangle. \quad (3.3)$$

We show the contribution of these two terms in Table IV. It is found that the first term $\{0p0h-2p2h\}$ is dominant and this result is consistent to the one in the old studies.¹⁾ We furthermore show each component in $\{0p0h-2p2h\}$ for the $l_{max} = 6$ case in Table V. Three configurations having large probabilities in Table III, give

Table II. The properties of ${}^4\text{He}$ for each l_{max} . We list the contributions from each term in the Hamiltonian and H_G (in units of MeV), the matter radii (R_m , in fm) and $P(D)$ (in %).

l_{max}	1	2	3	4	5	6
E	-22.66	-33.82	-40.85	-43.65	-44.55	-44.85
$\langle T \rangle$	66.77	82.25	90.53	91.83	92.08	92.16
$\langle V_C \rangle$	-68.59	-75.57	-79.16	-79.46	-79.43	-79.40
$\langle V_T \rangle$	-21.65	-41.17	-52.80	-56.52	-57.67	-58.06
$\langle V_{LS} \rangle$	-0.67	-0.20	-0.30	-0.36	-0.39	-0.40
$\langle V_{Cmb} \rangle$	0.87	0.87	0.88	0.87	0.86	0.86
R_m	1.34	1.27	1.24	1.24	1.24	1.24
$P(D)$	4.66	6.78	7.73	7.82	7.85	7.83
$\langle H_G \rangle / (1.5\hbar\omega)$	1.067	1.048	1.024	1.021	1.017	1.016

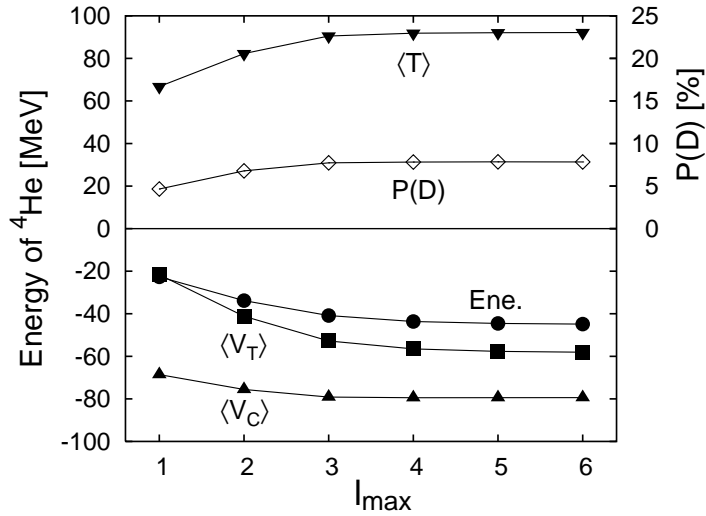


Fig. 1. Convergence of the properties of ${}^4\text{He}$ with respect to the l_{max} .

large contributions to $\langle V_T \rangle$, about 70% of the total value as shown in Table V. This means that three configurations are essential for the tensor correlation in ${}^4\text{He}$. When we increase the high partial waves from $l_{max}=3$ to 6, these configurations are kept mixed strongly. This result indicates that the $l_{max}=3$ case is enough to describe the characteristics of the configuration mixing for the tensor correlation in ${}^4\text{He}$.

3.2. Special feature and the strong shrinkage of the tensor correlation

We discuss the reason why three configurations are related to the tensor correlation. We illustrate the coupling scheme by the tensor force for the $0p0h$ and these $2p2h$ configurations in Fig. 2, where $\{l_i\}$ and $\{s_i\}$ ($i = 1, \dots, 4$) are the orbital angular momenta and the directions of the intrinsic spins for each nucleon in ${}^4\text{He}$, respectively. The $0p0h$ configuration of $(0s)^4$ is expressed as $1/\sqrt{2} \{ (0s_{1/2})_{01}^2 (0s_{1/2})_{01}^2 + (0s_{1/2})_{10}^2 (0s_{1/2})_{10}^2 \}$. When the tensor force acts on the $(0s_{1/2})_{10}^2$ in the $0p0h$ configuration, it changes the orbital angular momentum (L) and intrinsic spin (S) for excited particle states both by 2 ($\Delta L = 2$ and $\Delta S = 2$). The direction of ΔL and ΔS must be anti-parallel to each other since the rank of the tensor operator $S_{12} \propto [Y_2, [\sigma^1, \sigma^2]_2]_0$ is zero. The direction of S in the particle states of the $2p2h$ configuration is also opposite to that of the original $(0s_{1/2})_{10}^2$ component in the $0p0h$ case. If the $L = 2$ component in the $2p2h$ configuration consists of $l_3 = l_4 = 1$ for orbital angular momenta of excited two nucleons as shown in Fig. 2, the directions of the orbital angular momentum and the spin for each excited single-particle state are opposite and hence this state

Table III. The configuration of ${}^4\text{He}$ in the order of the probabilities in % for each case.

$l_{max}=1$		$l_{max}=2$		$l_{max}=3$	
$0p0h$	91.61	$0p0h$	89.38	$0p0h$	88.53
$(0p_{1/2})_{10}^2$	6.16	$(0p_{1/2})_{10}^2$	4.31	$(0p_{1/2})_{10}^2$	3.82
$(0p_{3/2})_{10}^2$	1.25	$(1s_{1/2})(0d_{3/2})_{10}$	3.00	$(0p_{3/2})(0f_{5/2})_{10}$	2.31
$(0p_{1/2})_{01}^2$	0.55	$(0d_{3/2})_{10}^2$	0.79	$(1s_{1/2})(0d_{3/2})_{10}$	2.03
$(0p_{3/2})_{01}^2$	0.37	$(0p_{3/2})_{10}^2$	0.75	$(0p_{3/2})_{10}^2$	0.57
$(0p_{1/2})(0p_{3/2})_{10}$	0.07	$(0d_{5/2})_{10}^2$	0.41	$(0d_{3/2})_{10}^2$	0.54
$l_{max}=4$		$l_{max}=5$		$l_{max}=6$	
$0p0h$	88.47	$0p0h$	88.45	$0p0h$	88.48
$(0p_{1/2})_{10}^2$	3.62	$(0p_{1/2})_{10}^2$	3.58	$(0p_{1/2})_{10}^2$	3.56
$(1s_{1/2})(0d_{3/2})_{10}$	2.03	$(1s_{1/2})(0d_{3/2})_{10}$	2.03	$(1s_{1/2})(0d_{3/2})_{10}$	2.03
$(0p_{3/2})(0f_{5/2})_{10}$	1.92	$(0p_{3/2})(0f_{5/2})_{10}$	1.90	$(0p_{3/2})(0f_{5/2})_{10}$	1.90
$(0d_{5/2})(0g_{7/2})_{10}$	0.61	$(0d_{3/2})_{10}^2$	0.54	$(0d_{3/2})_{10}^2$	0.54
$(0d_{3/2})_{10}^2$	0.54	$(0d_{5/2})(0g_{7/2})_{10}$	0.51	$(0d_{5/2})(0g_{7/2})_{10}$	0.52

Table IV. Expansion of $\langle V_T \rangle$ into two terms in Eqs. (3-1) in unit of MeV.

l_{max}	1	2	3	4	5	6
$0p0h$ - $2p2h$	-21.02	-42.03	-54.74	-59.25	-60.70	-61.22
$2p2h$ - $2p2h$	-0.63	0.86	1.94	2.73	3.03	3.16

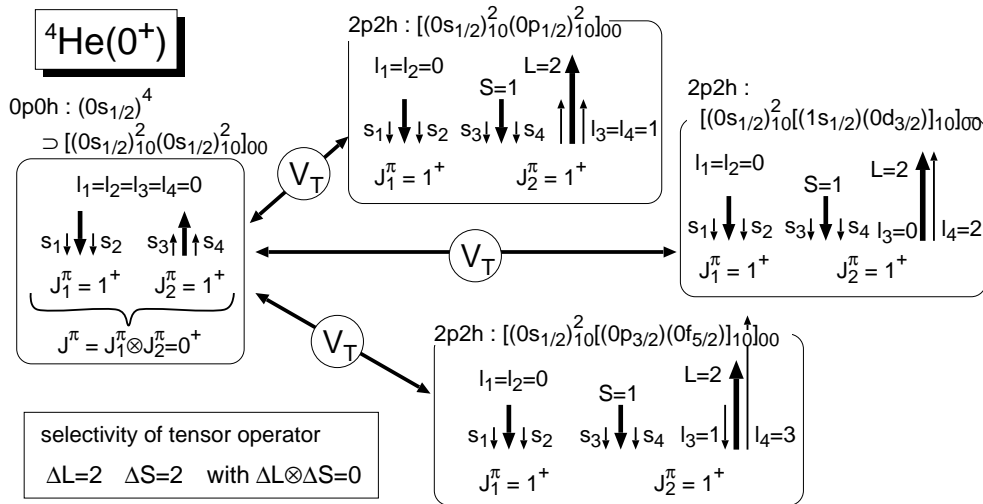
Table V. Contributions of each $0p0h$ - $2p2h$ coupling to $\langle V_T \rangle$ in MeV for the $l_{\max}=6$ case.

$2p$	$\langle \Phi_{0p0h} V_T \Phi_{2p2h} \rangle$
$(0p_{1/2})_{10}^2$	-14.47
$(1s_{1/2})(0d_{3/2})_{10}$	-15.01
$(0p_{3/2})(0f_{5/2})_{10}$	-12.00
$(0d_{3/2})_{10}^2$	-3.67
$(0d_{5/2})(0g_{7/2})_{10}$	-5.17

becomes $0p_{1/2}$ and $(0p_{1/2})_{10}^2$ is formed. This discussion is also understood as the 0^- coupling between $0s_{1/2}$ and $0p_{1/2}$ states in the particle-hole picture.^{12)–14)} If the $L=2$ component consists of $l_3=0$ and $l_4=2$, the directions of l_4 and spin for the single-particle state are also opposite, which become $0d_{3/2}$. This component makes $[(1s_{1/2})(0d_{3/2})]_{10}$ as shown in Fig. 2. If $l_3=1$, $l_4=3$, $[(0p_{3/2})(0f_{5/2})]_{10}$ is obtained in the similar way. Higher configurations having a set of larger orbital angular momenta of l_3 and l_4 show small amplitudes due to their large kinetic energies. As a result, the strong mixing of three $2p2h$ configurations in ${}^4\text{He}$ is understood from the selectivity of the operator of the tensor force.

We here discuss the relation of the spatial shrinkage of the single-particle states and the higher shell effect. For this purpose, we expand the shrunk single-particle wave function in terms of HOWF with the same length parameter of the $0s$ state. We calculate the accumulative probability defined as the summation of the expansion probabilities up to the quanta $N=2n+l$. The results are shown in Fig. 3 for the $l_{\max}=4$ case. The higher shell effect is seen as $2p2h$ configurations needed at least about $14\hbar\omega$ excitations for the shrunk states

In Fig. 4, we show the length parameter dependence of the solutions of ${}^4\text{He}$ in order to see the effect of the spatial shrinkage more clearly, where the length

Fig. 2. Schematic illustration of the favored coupling by the tensor force for ${}^4\text{He}$.

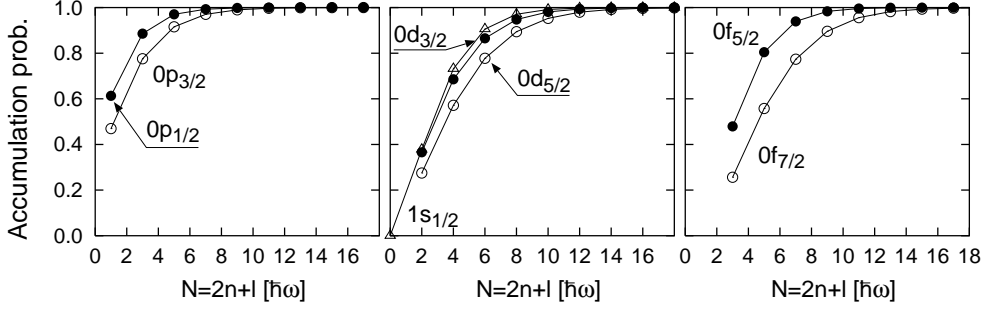


Fig. 3. Accumulative probabilities of the single-particle states for ${}^4\text{He}$ in terms of HOWF for the $l_{\max}=4$ case.

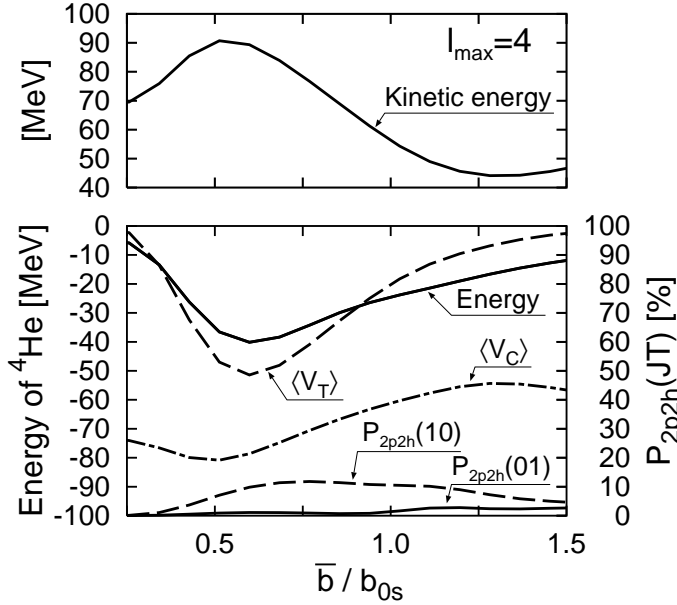


Fig. 4. The properties of ${}^4\text{He}$ in the $l_{\max}=4$ case as a function of \bar{b}/b_{0s} . $P_{2p2h}(JT)$ are the probabilities of $2p2h$ components with JT being the spin-isospin pair of the excited two nucleons.

parameters except for b_{0s} are changed as a common value \bar{b} . We plot the solutions as a function of the length parameter ratio \bar{b}/b_{0s} in the $l_{\max}=4$ case, where b_{0s} is fixed as 1.16 fm. The energy minimum is obtained at $\bar{b} \approx 0.6 b_{0s}$, where $\langle V_T \rangle$ gives the largest contribution and the kinetic energy becomes its maximum value. In comparison to the ordinary shell model case with $\bar{b}/b_{0s}=1$, $\langle V_T \rangle$ gains more than two times at the energy minimum point. For the $2p2h$ configurations, the $(J, T) = (1, 0)$ pair are strongly mixed around the energy minimum. From these results, the tensor force is incorporated with a small length parameter for the excited nucleon states.

As shown in Table I, the obtained wave functions give a smaller matter radii than the experimental value (1.48 fm) by 0.2 fm. This is due to the fact that in addition to the overbinding of the system, the length parameters of all single-particle states

are smaller than the case of the single configuration of $(0s)^4$ for ${}^4\text{He}$ with $b_{0s}=1.4$ fm, which reproduces the observed matter radii without the tensor correlation.

§4. Detailed analysis of the radial wave functions

In this section, we improve the radial wave functions of the particle states with the Gaussian expansion technique in order to achieve quantitative description of the tensor correlation. We adopt the Gaussian expansion method^{17),18)} for every excited particle states. This technique is shown to have wide applicability to describe the short-range correlation in few-body calculations and weakly bound states in neutron-rich nuclei.

We show the results in the $l_{\max}=2$ case. Here, we fix b_{0s} as 1.4 fm to give the appropriate matter radius of ${}^4\text{He}$ in the present wave function, since the results in Table II show too small a radius. We use a common number of basis functions, N_α , for every α of the particle states. The set of the length parameters of Gaussian bases in Eq. (2.1) are shown in Table VI.

From Fig. 5, we confirm a good convergence of the solutions with respect to N_α . In particular, the physical quantities almost converge within three or four bases, where the bases with smaller length parameters than b_{0s} are favored. It is also found that the Gaussian expansion gives a larger effect on $\langle V_T \rangle$ than $\langle V_C \rangle$. In particular, $P(D)$ becomes the value around two times of the single Gaussian case ($N_\alpha = 1$). The kinetic energy also increase about 20% in the Gaussian expansion from the $N_\alpha = 1$ case. The matter radius converges in 1.39 fm. As a result, the Gaussian expansion succeeds in describing the radial wave functions for the excited particle states and increases the tensor correlation for ${}^4\text{He}$. In order to estimate this effect, we calculate

Table VI. The set of the length parameters for Gaussian basis functions.

N_α	set of $b_{\alpha,m}$ ($m = 1, \dots, N_\alpha$)
1	0.7
2	0.6 0.8
3	0.6 0.8 1.0
4	0.6 0.8 1.0 1.4
5	0.6 0.8 1.0 1.4 2.0
6	0.4 0.6 0.8 1.0 1.4 2.0
7	0.4 0.6 0.8 1.0 1.4 2.0 2.5

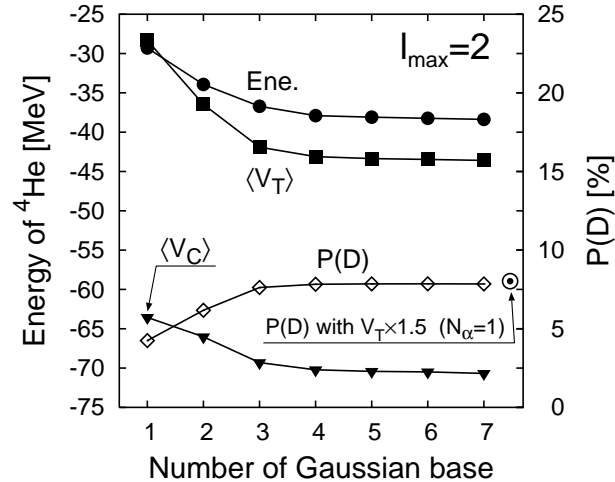


Fig. 5. The properties of ${}^4\text{He}$ with Gaussian expansion method. Circle indicates $P(D)$ with a single Gaussian basis with increasing the matrix element of the tensor force by 50%.

^4He with the single Gaussian basis. If we enhance the matrix elements of the tensor force by 50%, the result of the Gaussian expansion is simulated.

§5. Properties of ^4He with tensor force of the nucleon-nucleon force

In this section we provide the results with TOSM for ^4He using the tensor force of the nucleon-nucleon interaction together with the central interaction modified by taking care of the short-range repulsion. For this purpose, we first compare the matrix elements of the tensor forces obtained in various methods.

5.1. The matrix elements of various tensor forces

We compare the radial matrix elements of the tensor force $V_T = f_T(r) \cdot S_{12}$, in the several interactions; The bare nucleon-nucleon interaction, AV8',²²⁾ and the Bonn potential with $\pi + \rho$ ²³⁾, and G -matrix tensor interaction, AK, which is based on AV8'. In Fig. 7, we show the radial dependence $f_T(r)$ of each tensor force for triplet-even channel. We see that the short-range behaviour depends very strongly on the choices of the nucleon-nucleon interaction. On the other hand, the medium- and long-range behaviours are very similar each other.

We compare now the radial integrals of three kinds of the tensor forces for the S - D coupling in the relative motion defined by the following equations.

$$I_{SD} = \int_0^\infty dr M_{SD}(r), \quad M_{SD}(r) = r^2 \phi_{0s}(r, b_{0s}) \cdot f_T(r) \cdot \phi_{0d}(r, b_{0d}). \quad (5.1)$$

This matrix element is essential to describe explicitly the tensor correlation. Here, ϕ_{0s} and ϕ_{0d} are the radial components of the Gaussian wave functions for s and d waves with length parameters of b_{0s} and b_{0d} , respectively. We take $b_{0s} = 1.4 \cdot \sqrt{2}$ fm for the $0s$ wave function where the factor $\sqrt{2}$ comes from the relative coordinate transformation of HOWF. We take two length parameters, $b_{0d} = b_{0s}/2$ and $b_{0d} = b_{0s}$ for the $0d$ wave function. The smaller length parameter of b_{0d} corresponds to the case of the biggest matrix element of the tensor force as discussed in the previous sections and the previous study¹⁵⁾ and the larger length parameter corresponds to the case of the tensor force in the standard shell model.

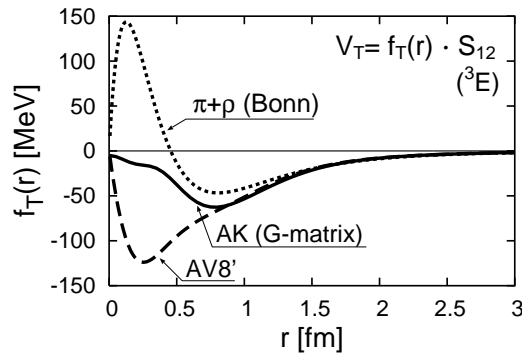
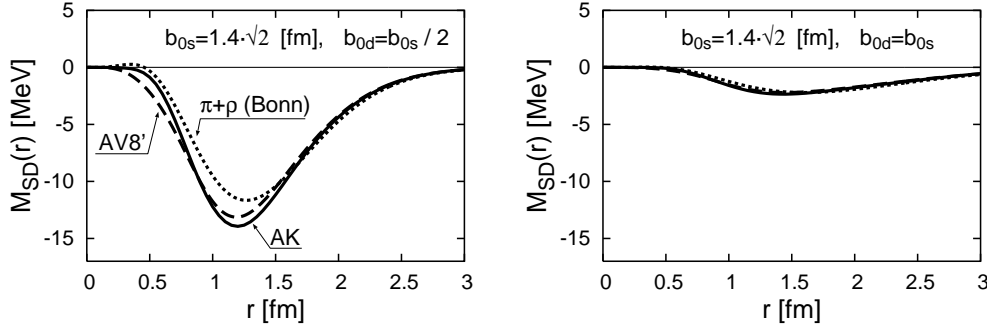


Fig. 6. Comparison of the tensor forces for triplet-even channel.

Fig. 7. Comparison of the integrand of the radial matrix elements of the tensor force with two b_{0d} .Table VII. Radial matrix elements of the tensor force I_{SD} for triplet-even channel. Unit in MeV.

	AV8'	AK	$\pi + \rho$ (Bonn)
$b_{0d} = b_{0s}/2$	-14.98	-15.04	-13.30
$b_{0d} = b_{0s}$	-3.83	-3.85	-3.82

In the left figure of Fig. 7, we show the shorter range case of the radial integrands $M_{SD}(r)$ of the three cases, which are very similar each other. The intermediate and long-range behaviour is important for the matrix element of the tensor force. The large difference in the short-range part is washed out due to the $\Delta L = 2$ transition of the tensor force for relative orbital angular momentum. Due to the centrifugal barrier of D state, contribution from short-range part becomes small in the tensor-force matrix elements. This means that the coupling between the short-range correlation and the tensor correlation is weak, so that we can describe the tensor correlation explicitly in the shell model type method while we can renormalize the short-range correlation into the central force independently from the tensor force. In the right figure of Fig. 7, we also show the longer range case. Here, again the radial integrands are very similar. We show further the matrix elements of each tensor force, I_{SD} , in Table VII. We find that the three matrix elements come out to be very similar within 10%. We also see the tensor matrix element of the shorter length parameter is much larger than the case of that with the tensor matrix element of the larger length parameter, which corresponds to the case of the standard shell model.

5.2. The properties of ${}^4\text{He}$ in TOSM

We have studied the full treatment of the tensor force in the shell model type method by taking enough angular momenta and also the radial wave functions using the V -type coordinates. There we have taken the effective nucleon-nucleon interaction, GA. We have found good convergence with medium angular momenta with a few range parameters for the tensor force. Since this is the first time to treat the tensor force fully while the short-range repulsion has to be treated somehow at the present, the binding energy of ${}^4\text{He}$ comes out too large and also the size of ${}^4\text{He}$ too small. Here, we would like to readjust the parameters of the central interaction so that the properties of ${}^4\text{He}$ comes out good. In the previous subsection, in addition,

Table VIII. The properties of ${}^4\text{He}$ in the $l_{\max}=5$ case with the use of the bare tensor force. We list the contributions from each term in the Hamiltonian (in unit of MeV) and the matter radius (R_m , in fm) and the probabilities (in %) of each configuration labeling with the excited particle states.

E	-27.89	$P(D)$	9.13
$\langle T \rangle$	75.85	$0p0h$	85.02
$\langle V_C \rangle$	-44.57	$(0p_{1/2})_{10}^2$	3.40
$\langle V_T \rangle$	-58.97	$(1s_{1/2})(0d_{3/2})_{10}$	2.35
$\langle V_{LS} \rangle$	-0.98	$(0p_{3/2})(0f_{5/2})_{10}$	2.21
$\langle V_{Cmb} \rangle$	0.78	$(0p_{1/2})(0p_{3/2})_{10}$	1.61
$\langle H_G \rangle / (1.5\hbar\omega)$	1.011	$(0d_{5/2})(0g_{7/2})_{10}$	0.83
R_m	1.47	$(0d_{3/2})_{10}^2$	0.60
		$(0p_{3/2})_{10}^2$	0.53

we have shown that we are able to treat the bare tensor force obtained from the nucleon-nucleon scattering and the matrix elements of tensor forces come out to be very similar due to the large centrifugal potential. Hence, we take the bare tensor force for the study of ${}^4\text{He}$ and take a phenomenological central interaction in TOSM.

We adopt the tensor force and the LS force of AV8'. As for the central interaction we base on the central force of the GPT interaction, which is obtained by fitting the observed two-nucleon properties. We furthermore adjust the central part of GPT to improve the large binding energy as explained in Table II. This is carried out by reducing the strength of the second range (attractive part) of GPT's central force by 13% in order to fit the observed binding energy (28.3 MeV) for ${}^4\text{He}$.

For the ${}^4\text{He}$ wave function, we take $l_{\max}=5$ for high angular momentum states and take four Gaussian basis functions for every particle state, whose length parameters are 0.6, 0.8, 1.0 and 1.4 fm, respectively. These choices are sufficient in the present calculation. For the $0s$ state, we determine its length parameter variationally, obtained as 1.42 fm.

The results for ${}^4\text{He}$ are shown in Table VIII. For mixing probabilities, we sum up the probabilities belonging to the same configurations having the same spin and isospin pair with different radial components obtained in the Gaussian expansion. It is found that $\langle V_T \rangle$ is about -60 MeV and $P(D)$ reaches about 9%. These results mean that the obtained wave function satisfactorily represents the characteristics of the tensor correlations. The excitation of the spurious c. m. motion is weak and its amount is estimated as around 0.4 MeV. Three $2p2h$ configurations are strongly mixed and $(0p_{1/2})_{10}^2$ component is most favored.

§6. Summary

We have studied the tensor correlation in ${}^4\text{He}$ in the shell model type method with the use of the V -type coordinate. We have developed the tensor optimized shell model (TOSM) to treat fully the tensor correlation. We have applied the TOSM to ${}^4\text{He}$, where we take the $(0s)^4$ basis and include up to the two-particle two-hole ($2p2h$)

excitations with particle states up to medium angular momenta. Particle states are expressed in terms of Gaussian wave functions for each partial wave, while the length parameters are allowed to change so as to minimize the total energy. For the study of the tensor correlation we have taken first the G -matrix interaction based on the AV8' interaction^{19),20)} and replace the central part of the interaction by those of the GPT.²¹⁾

We have first of all calculated ${}^4\text{He}$ by including the medium high angular momentum states up to l_{max} successively, while employing only one Gaussian basis function for each orbit. We have found that the spatial size of the particle states are largely shrunk in order to optimize the tensor correlation for ${}^4\text{He}$. The Gaussian length parameters of high partial waves come out to be about 60 % of that of $0s$ state. The energy gain from the tensor force increases largely with increasing l_{max} and shows the convergence around $l_{max} \sim 4$. We have found three particular $2p2h$ states admix to the $(0s)^4$ component due to the characteristic feature of the tensor force. We have then expressed the radial wave function in terms of the superposition of the Gaussian basis functions with several length parameters. We have found that about three Gaussian basis functions are sufficient to express the radial wave functions and the energy gain due to the use of various Gaussian wave functions is about 50% than the case of one Gaussian wave function. Hence, we have succeeded to develop the shell model type model based on the V -type coordinate, TOSM, which is able to treat the strong tensor force.

We have then studied ${}^4\text{He}$ with TOSM by using the bare tensor force, AV8', and the short-range modified central interaction, GPT. We are able to calculate the ground state properties of ${}^4\text{He}$ with a modification of the medium-range of GPT central interaction so as to reproduce the binding energy. The expectation value of the tensor force is very large, about -60 MeV and the D -state probability is about 10%.

We have developed the TOSM, where we are able to treat the bare tensor force, with the hope to investigate the tensor correlations in heavy nuclei. As the next step we ought to develop a method to handle the short-range repulsion so that we are able to treat medium and heavy nuclei using the nucleon-nucleon interaction. We shall also study the effects of the tensor correlation on the structures of the neighboring nuclei of ${}^4\text{He}$. Particularly interesting is the scattering phenomena of the ${}^4\text{He}$ +neutron system ($A = 5$) and the structures of $A = 6$ system, ${}^6\text{He}$, ${}^6\text{Li}$ and ${}^6\text{Be}$.

Acknowledgements

The authors would like to thank Prof. Horiuchi and Prof. Yamada for fruitful discussions and encouragement. This work was supported by the Grant-in-Aid for Japan Society for the Promotion of Science(JSPS, No. 18-8665) and the 21st Century COE program. This work was performed as a part of the Research Project for Study of Unstable Nuclei from Nuclear Cluster Aspects (SUNNCA) in RIKEN. Numerical calculations were performed in the computer system of RCNP.

References

- 1) Y. Akaishi, Int. Rev. of Nucl. Phys. **4**(1986), 259.
- 2) A. Nogga, H. Kamada and W. Glöckle, Phys. Rev. Lett. **85** (2000), 944.
- 3) H. Kamada *et al.*, Phys. Rev. C **64** (2001), 044001.
- 4) R. B. Wiringa, S. C. Pieper, J. Carlson and V. R. Pandharipande, Phys. Rev. C **62** (2000), 014001.
- 5) H. Mütter and A. Polls, Prog. Part. Nucl. Phys. **45** (2000), 243.
- 6) Y. Akaishi, H. Bandō and S. Nagata, Prog. Theor. Phys. Suppl. No. 52 (1972), 339.
- 7) K. Andō, H. Bandō, S. Nagata, Y. Akaishi, E. M. Krencliglowa, T. Sakuda, F. Nemoto, T. Motoba, K. Itonaga, Y. Yamamoto, M. Kohno, N. Yamaguchi, Prog. Theor. Phys. Suppl. No. 65 (1979), .
- 8) K. Ando, H. Bando, Prog. Theor. Phys. **66** (1981), 227.
- 9) H. Nakada, Phys. Rev. C **68** (2003), 014316.
- 10) T. Neff and H. Feldmeier, Nucl. Phys. A **713** (2003), 311.
- 11) H. Feldmeier, T. Neff, R. Roth, J. Schnack, Nucl. Phys. A **632** (1998), 61.
- 12) H. Toki, S. Sugimoto and K. Ikeda, Prog. Theor. Phys. **108** (2002), 903.
- 13) Y. Ogawa, H. Toki, S. Tamenaga, H. Shen, A. Hosaka, S. Sugimoto and K. Ikeda, Prog. Theor. Phys. **111** (2004), 75.
- 14) S. Sugimoto, K. Ikeda and H. Toki, Nucl. Phys. A **740** (2004), 77.
- 15) T. Myo, K. Katō and K. Ikeda, Prog. Theor. Phys. **113** (2005), 763.
- 16) K. Shimizu, M. Ichimura and A. Arima, Nucl. Phys. A **226** (1973), 282.
- 17) E. Hiyama, Y. Kino and M. Kamimura, Prog. Part. Nucl. Phys. **51** (2003), 223.
- 18) S. Aoyama, S. Mukai, K. Katō and K. Ikeda, Prog. Theor. Phys. **93** (1995), 99.
- 19) Y. Akaishi, Nucl. Phys. A **738** (2004), 80.
- 20) K. Ikeda, S. Sugimoto and H. Toki, Nucl. Phys. A **738** (2004), 73.
- 21) D. Gogny, P. Pires and R. De Tourreil, Phys. Lett. B **32** (1970), 591.
- 22) B. S. Pudliner, V. R. Pandharipande, J. Carlson, S. C. Pieper and R. B. Wiringa, Phys. Rev. C **56** (1997), 1720.
- 23) R. Machleidt, Phys. Rep. **149**(1987), 1.